On pair additivity of the depletion force

2003 J. Phys.: Condens. Matter 15 8281

(http://iopscience.iop.org/0953-8984/15/49/007)

INSTITUTE OF PHYSICS PUBLISHING JOURNAL OF PHYSICS: CONDENSED MATTER

J. Phys.: Condens. Matter **15** (2003) 8281–8290 PII: S0953-8984(03)62796-7

On pair additivity of the depletion force

Dengming Zhu, Weihua Li and H R Ma

Institute of Theoretical Physics, Shanghai Jiao Tong University, Shanghai 200240, People's Republic of China

Received 25 April 2003, in final form 8 October 2003
Published 25 November 2003
Online at stacks.iop.org/JPhysCM/15/8281

Abstract

The depletion interaction between two and three big hard spheres in a small hard sphere fluid with volume fraction $\pi/10$ is calculated both from Monte Carlo simulations and the Asakura–Oosawa approximation. The Monte Carlo results are in good agreement with previous DFT results. The three-body interaction at this volume fraction of small hard spheres is found to be very small, which indicates that the pair additivity of the depletion force is a good approximation.

1. Introduction

Since the pioneering work of Asakura and Oosawa (AO) [1] on the entropic forces between colloidal particles in polymer colloid suspension systems, there has been continuing interest in the studies of the depletion effects in different systems. Recently, there are renewed interests in this effect as a result of advancement in new observation methods and theoretical tools. Measurements of depletion forces are accessible in recent years either by scattering methods [2, 3] or by direct methods [4–7]. Many theoretical investigations on the depletion interactions by means of integral equation methods and simulation methods have also been reported [8–11]. Dijkstra *et al* gave a systematic treatment of a highly asymmetric binary hard sphere system [12]; they obtained the phase diagram of the system by first integrating out the small hard sphere component and did calculations on the large hard sphere system with an effective interaction which includes the depletion effects up to a two-body term, with the higher-body interactions being neglected. The pair force between two big spheres of a two-component colloidal system was calculated by different methods. The structure of the colloidal system based on the depletion pair forces has also been studied by different methods. In all these researches the pair additivity of the depletion force was assumed. The origin of the depletion force comes from the entropy of the system as a whole; it is natural to expect that the interaction is not necessarily pair-additive. It was argued by Biben *et al* [8] based on the superposition approximation that the many-body force is negligibly small. Brader *et al* [13] studied a colloid–polymer mixture, and found that the many-body depletion interaction between colloid particles is absent when the size ratio of the polymer coil and colloid is less then $2/\sqrt{3} - 1 \approx 0.1547$. The three-body depletion interaction was calculated recently by Goulding and Melchionna [14] from density functional theory; they used the widely accepted

0953-8984/03/498281+10$30.00

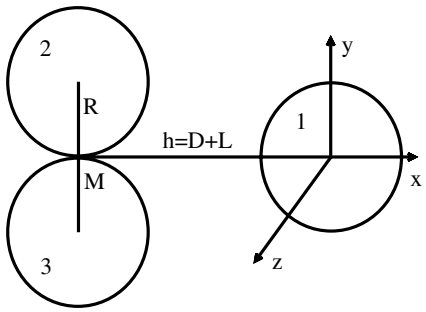

Figure 1. The configuration of three big spheres. M is the touching point of the spheres 2 and 3, h is the distance between the centre of sphere 1 and point M, $L = \sqrt{3}R$ is the smallest h when sphere 1 is in touch with sphere 2 and 3.

Rosenfeld [15] functional and obtained the three-body depletion potential through functional differentiation. Their results indicated that the three-body interaction is indeed much smaller then the two-body interaction. It was proven that density functional theory gives accurate results in two-body depletion interactions; it is not justified that this should be true in three-body interaction calculations. In this paper we will investigate the three-body interaction by the simple AO approximation as well as Monte Carlo simulation. Our result is similar to that of the DFT calculations, thus confirming that DFT can give highly accurate results in the evaluation of three-body depletion interactions and justifying the validity of many studies based on simple pairwise interactions.

2. Theory and methods

The model in this study is a system of three big hard spheres immersed in a small hard sphere fluid. By calculating the effective interactions between the big spheres due to the depletion effect of the small spheres, we extract the three-body force from the calculation.

In a fluid of small spheres in an external potential composed of two contributions, one from any fixed obstacle and the other from a fixed big sphere, the force on the big sphere is given by [16, 17]

$$F = -k_{\mathrm{B}}T \int_S \rho(\mathbf{r})\hat{\mathbf{n}}\,\mathrm{d}S, \tag{1}$$

where the integral is over the surface S of a sphere of radius $R + a$ centred on the centre of the big sphere under consideration, R is the radius of the big sphere and a is the radius of a small sphere. k_{B} is the Boltzmann constant, T the absolute temperature, $\hat{\mathbf{n}}$ the outward normal unit vector of the sphere surface and $\rho(\mathbf{R})$ the local density of small spheres. This formula was derived and used by many authors for the studies of the depletion interaction of two big hard spheres [16, 17], and the interaction between a big hard sphere and a planar hard wall [16]. As pointed out by Götzelmann *et al* [16], the formula is valid for any kind of fixed obstacles. From (1) we know that the force on the big hard sphere was determined by local small sphere densities around the big sphere, i.e. when the density of the small spheres is determined by some means, the force can readily be obtained from a simple integration.

Due to the mass calculation resources required in simulation, we will study in this paper only the special arrangement of three big spheres shown in figure 1, immersed in a fluid of small hard spheres, where two big spheres (labelled as 2 and 3 in the figure) are held fixed and in contact; M is the touching point. The third (labelled 1) is in front of the two big spheres, with the line connecting its centre and point M perpendicular to the line connecting spheres 2

and 3. h is the distance between sphere 1 and point M, which is represented as $D + L$, with $L = \sqrt{3}R$ the distance between M and the centre of sphere 1 when the three spheres are in contact. The three-body force on big sphere 1 is defined as

$$\mathbf{F}^{(3)} = \mathbf{F}_1 - \mathbf{F}_{12} - \mathbf{F}_{13}, \tag{2}$$

where $\mathbf{F}_1$ is the total force on the big sphere 1, $\mathbf{F}_{12}$ is the force on sphere 1 when sphere 3 is absent, and $\mathbf{F}_{13}$ is the force on sphere 1 when sphere 2 is absent. Similarly the three-body depletion potential on sphere 1 is defined as

$$W^{(3)} = W_1 - W_{12} - W_{13}, \tag{3}$$

where the W are the depletion potentials with the subscripts having the same meaning as in the case of the depletion forces.

First, we discuss the three-body force from the AO model [1]. In this model one approximates the small sphere density around the big sphere as the bulk density if the region is allowed for the small sphere to enter and zero if it is forbidden. From the symmetry of the configuration considered here (see figure 1) the forces on sphere 1 along the y direction and the z direction are zero. The two-body forces F_{12} and F_{13} in this approximation are given by [1]

$$F_{1i}(D) = \begin{cases} -\dfrac{3KT\eta}{4a^3}\left(R + \dfrac{1}{2}a + \dfrac{1}{4}D_{1i}\right)(2a - D_{1i}) & D_{1i} < 2a \\ 0 & \text{otherwise.} \end{cases} \tag{4}$$

The force F_{1i} is along the line connecting sphere 1 and i. Here $i = 2, 3$ represents big spheres 2 and 3, D_{1i} is the separation of big sphere 1 and big sphere i, and the minus sign means the force is attractive. η is the volume fraction of small sphere fluid; it is related to the density of the small sphere fluid ρ by $\eta = \frac{4}{3}\pi a^3\rho$. The total force on sphere 1 in the configuration in figure 1 can be derived as (see appendix)

$$F_1 = \begin{cases} -\dfrac{3kT}{4a^3}\eta\dfrac{4(R+a)^2h^2 - (R^2+h^2)^2}{4h^2} + \dfrac{3kT}{a^3}\eta(R+a)^2J & L \leqslant h \leqslant L_1 \\ -\dfrac{3kT}{2a^3}\eta(R+a)^2\left(1 - \dfrac{R^2+h^2}{4(R+a)^2}\right)\dfrac{h}{\sqrt{h^2+R^2}} & L_1 < h \leqslant L_2 \\ 0 & h > L_2, \end{cases} \tag{5}$$

with $L = \sqrt{3}R$, $L_1 = (R + a) + [(2R + a)a]^{1/2}$, $L_2 = [(R + 2a)(3R + 2a)]^{1/2}$, where

$$J = \int_{\theta_1}^{\theta_2} \sin\theta\cos\theta\left(\frac{\pi}{2} - \arcsin\left(\frac{h^2 + R^2 + 2(R+a)h\cos\theta}{2R(R+a)\sin\theta}\right)\right)\mathrm{d}\theta, \tag{6}$$

and θ_1 and θ_2 are

$$\begin{aligned} \theta_1 &= \arccos\frac{-h(h^2+R^2)^2 + [4(R+a)^2R^2 - R^2(R^2+h^2)]^{1/2}}{2(R+a)(R^2+h^2)^2} \\ \theta_2 &= \pi - \arccos\frac{R^2+h^2}{2h(R+a)}. \end{aligned} \tag{7}$$

The three-body force is zero when $h > L_1$, and when $L \leqslant h \leqslant L_1$ is given by

$$\begin{aligned} F^{(3)} = &-\frac{3kT}{4a^3}\eta\frac{4(R+a)^2h^2 - (R^2+h^2)^2}{4h^2} \\ &+ \frac{3kT}{a^3}\eta(R+a)^2J + \frac{3kT}{2a^3}\eta(R+a)^2\left(1 - \frac{R^2+h^2}{4(R+a)^2}\right)\frac{h}{\sqrt{h^2+R^2}}. \end{aligned} \tag{8}$$

Figure 2 is a plot of the force on sphere 1 as function of D. When $L_1 \leqslant L$, the three-body interaction is absent. By equating L_1 with L, the condition that the three body force is absent can be obtained as $a/R \leqslant 2/\sqrt{3} - 1 \approx 0.1547$, in agreement with the result from [13].

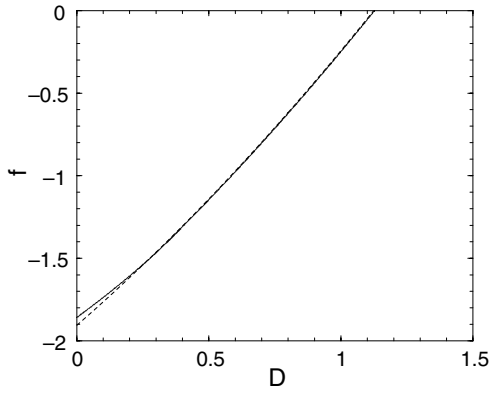

Figure 2. The calculated force on sphere 1 of three big spheres (solid curve) and the pair-added force (dashed curve) by AO approximation as a function of D. $D = 0$ means that the three spheres are in contact.

The AO approximation usually gave quantitatively poor results of the depletion forces in hard sphere systems. In order to get more reliable information of the three-body interaction, Monte Carlo simulation is performed in this study. The method used here is the acceptance ratio method (ARM), which was first proposed by Bennett [18], and implemented in the case of hard particle systems by Li *et al* and used in the studies of depletion interactions of different systems [19–21]. Details of the ARM method and its implementation can be found in [18, 20]. We calculated the depletion potentials between two big hard spheres and the depletion potential on the big hard sphere 1 in the configuration shown in figure 1. The *three-body* depletion potential $W^{(3)}$ is then obtained by subtracting the two-body potentials from the full three big hard sphere result, as given in equation (3).

In our simulations we used the diameter of a small sphere as the unit of length so that its radius is $a = 0.5$; the big sphere radius is R, and the size ratio is defined as $\xi = a/R$. The volume fraction of the small sphere fluid is fixed at $\eta = \pi/10$. The simulation sample is a rectangular box of size $L_x \times L_y \times L_z$. Periodic boundary conditions were used in all three directions. In the calculation of the depletion interaction between two big spheres, the separation of the two spheres is changed and free energy differences between different distances of the two spheres are obtained; by fixing the zero point of potential to a reference point we obtain the depletion potential. In the case of three big hard spheres, the distance between the midpoint M and the centre of sphere 1 is $L = \sqrt{3}R = 4.34$ when the three spheres are in contact. We chose this point as the reference point in our calculation. The big spheres 2 and 3 were kept fixed during the simulation while sphere 1 was placed at different places in the x direction, ranging from contact to a larger distance. The depletion potential on sphere 1 is obtained from free energy differences of different places of sphere 1. The numbers of the small spheres used in the simulations are determined by the prescribed volume fractions and the size of the simulation box; typically 1649 small spheres are used in the two-body calculation and 2269 are used in the case of three big hard spheres.

3. Result and discussion

3.1. Result by AO theory

AO theory assumes that the small sphere density is constant where the small spheres can accommodate, and otherwise is zero. Under AO theory the scaled force (the force in units

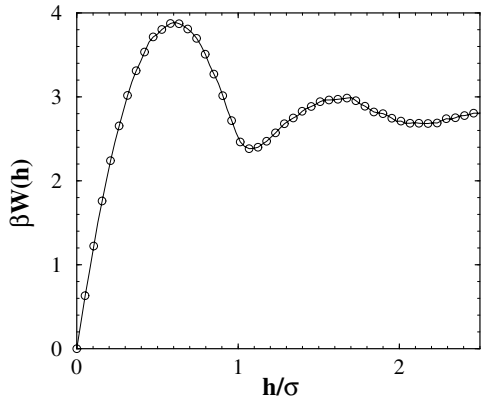

Figure 3. The simulated depletion potential between two big spheres. The points are simulated results and the curve is a smooth joining of the points through spline regression. h is the minimum surface to surface distance between two big spheres; the size ratio is $\xi = 0.2$.

of $R\pi\rho k_{\mathrm{B}}T$) is independent of the small sphere density. The force is only determined by the ratio of the radius of a small sphere and a big sphere. When $\xi = 0.2$, we see from figure 2 that the three-body potential is very small. When $\xi = 0.5$, the three-body potential given by AO approximation becomes significant, as indicated in figure 6. However, this effect comes from the AO approximation, which is valid only in the limit of low volume fractions of small hard spheres; it is not a real effect of the current physics model where the volume fraction of the small hard sphere is $\pi/10$.

3.2. Results by the simulation method

The two-body depletion potential obtained from simulation is shown in figure 3, which is exactly the same as a previous Monte Carlo simulation with a different method [9]. The simulation box used is $20 \times 12 \times 12$ and 1649 small spheres were used in the calculation. The volume fraction is $\pi/10$ and the size ratio $\xi = 0.2$. In figure 3 the symbols are simulated results, the statistical error and the error from finite size effects are estimated to be less then the size of the symbols. The curve is from a spline regression of the data points obtained from simulation.

In the case of three big hard spheres, the box size is $L_x = 19.50$, $L_y = 17.0$, $L_z = 12.0$. The big spheres are placed in the box as described above. When $\eta = \pi/10$ the number of small spheres is 2269 in the case $\xi = 0.2$. Figure 4 is the result of the depletion potential on big sphere 1; the solid curve is from direct simulation of full three big hard spheres and the dashed line is the superposition of the potentials from hard spheres 2 and 3. The two lines are very close to each other, which indicates that the depletion potential is indeed small.

Figure 5 is the three-body depletion potential obtained by equation (3) and the simulated depletion potentials of W_1, W_{12} and W_{13}. The results are shown in the figure as symbols, and the results from DFT calculation by Goulding and Melchionna [14] are shown as a solid curve; we also show the results from AO approximation as a dashed curve for comparison. The statistical errors of our simulation to the depletion potentials W_1, W_{12} and W_{13} are controlled to be less then 0.5%, and the finite size effect is very small compared to the statistical errors when h is smaller than 1.5 but becomes more and more important when h increases. In the inset of figure 4 the three sphere simulation for two different cell sizes are plotted; the two results are

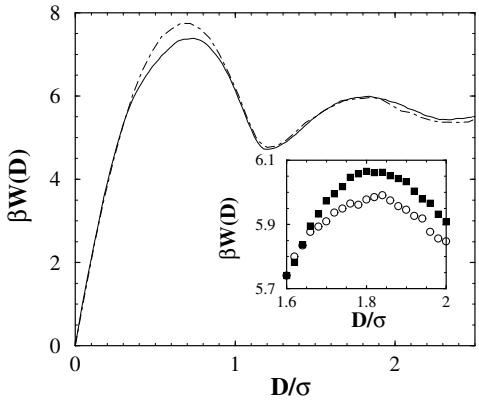

Figure 4. The simulated depletion potential on big sphere 1 as a function of D, defined in figure 1. The solid curve is the result of full three big spheres, the dashed curve is the superposition of the depletion potential from spheres 2 and 3; the size ratio is $\xi = 0.2$. Inset: the part of three big sphere simulation when sphere 1 is far from spheres 2 and 3 with two different sizes of simulation boxes, showing the finite size effect in our simulation. Squares are the results for cell $17.5 \times 15 \times 10$ and circles are for cell $L_x = 19.5 \times 17 \times 12$.

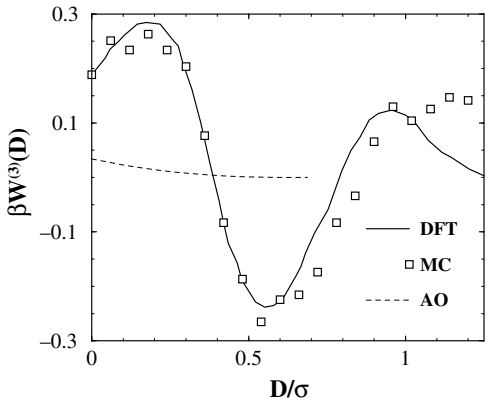

Figure 5. The three-body depletion potential as a function of D with size ratio $\xi = 0.2$; the dashed curve is from AO approximation, symbols are from simulation and the solid curve is from density functional theory calculation by Goulding and Melchionna [14]. The AO approximation underestimates the three-body depletion interaction in this case.

the same within statistical errors before $h = 1.5$, and deviate from each other after $h = 1.6$. Since the three-body depletion potential is obtained by the subtraction of two large numbers, the error of it is enhanced greatly. The error of the three-body depletion potential is estimated to be less than 15% when $h \leqslant 1.6$, and becomes less accurate after $h = 1.6$. Our simulation result is in good agreement with the DFT result as indicated by figure 5, which confirmed the DFT calculation and, more importantly, confirms that DFT can give accurate results not only to the two-body depletion potentials but also of three-body interactions. However, it can be seen clearly from the plot that AO approximation underestimates the three-body depletion interactions by a factor of about $1/6$.

Figure 6 is the simulated three-body depletion potential with size ratio $\xi = 0.5$, that is, the radius of the small sphere is half of the radius of the big sphere. The three body interaction

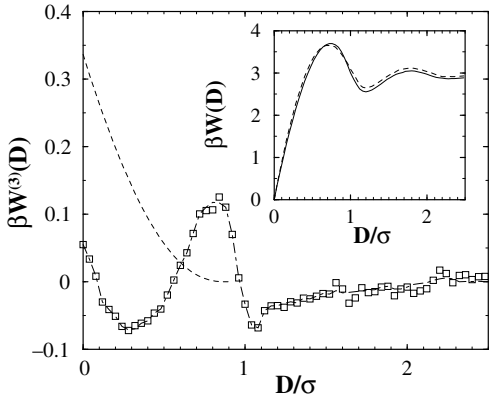

Figure 6. The three-body depletion potential as a function of D with size ratio $\xi = 0.5$. The dashed curve is from AO approximation, symbols are from simulation and the curve that connects the symbols is a guide to the eye. In this case the AO approximation overestimates the three-body depletion interaction. Inset: the simulated potential on big hard sphere 1 (solid curve) and the potential from superposition (dashed curve).

under the AO approximation is much larger than the previous case where $\xi = 0.2$, and in this case it overestimates the three-body depletion interaction by a factor of about 3. However, our simulation indicates that the three-body interaction is still small in this extreme case of anisotropy as clearly shown in figure 6; in fact, the absolute value of the three-body potential is even smaller than that when $\xi = 0.2$. The relative importance of the three-body depletion interaction in the two cases of different size ratios is comparable; both are less then 3.5% compared to the two-body superposition.

A closer look at the DFT calculation by Goulding and Melchionna [14] shows that the magnitude of the three-body depletion potential decreases with increasing size ratio when the volume fraction of the small spheres is large ($\eta = \pi/10$), and increases with increasing size ratio when the volume fraction of the small spheres is small ($\eta = \pi/30$). For even smaller volume fractions of the small spheres the results tend to the AO approximation as expected. Since our simulation confirms the DFT calculation in one case where the volume fraction of the small spheres is large, we believe that the DFT results are even more accurate for the smaller volume fractions of the small spheres.

By comparing figures 5 and 6, we see that the dependence of the three-body depletion potential on h is very different for different size ratios; this is in contrast to the two-body depletion interactions where the form is similar for different size ratios.

As we can see from our simulation and the DFT calculations by Goulding and Melchionna [14], the three-body depletion interaction is very small compared to two-body depletion interactions, and the additivity of a depletion potential is a very good approximation in the studies of systems of binary colloids with one small component averaged out. This also suggests that studies in the literature based on pair potentials are reliable. However, the many-body interactions, though small, have characteristic features which are not present in the two-body term. The form of the interaction is sensitive both to the volume fractions of small hard spheres and the size ratio of the spheres; though these features may have little effect in the liquid phase of the hard sphere system, they may play important parts in the phase separation and structure formation of the system. In a recent publication, Dijkstra and van Roij [22] studied the many-body depletion effects on wetting and many-body induced layering in a colloid–polymer mixture. This system can be described by the AO model in which the

interaction between polymer blends can be neglected. From our simulation calculation and the DFT calculation, in the case that the volume fraction of the small spheres is high, the many-body depletion interaction of a binary hard sphere system is weaker than that predicted by the AO model; we expect that the many-body effects should be weaker than those reported in [22].

In conclusion, we calculated the three-body depletion interaction of hard spheres in both AO approximation and Monte Carlo simulation at a high value of small hard sphere volume fraction $\pi/10$. The results indicate that the three-body interaction is small and pair additivity of the depletion force is a good approximation to the real depletion interaction in many cases. We also confirmed that the relative importance of the three-body depletion interaction is not sensitive to the size ratios of large and small hard spheres under high volume fraction of small hard spheres, as already indicated by the DFT calculations in [14]. Our Monte Carlo simulation results are close to the results of DFT based on the Rosenfeld functional, which confirms the accuracy of DFT in the three-body depletion potential calculation. Since the simulation requires heavy numerical computation while the numerical computation in DFT is relatively smaller, further investigations on three-body depletion effects can safely be performed in the DFT frame and sufficiently accurate results are expected. The AO approximation, as a simple and analytic manageable method, usually gives intuitively correct results for depletion effects especially in the case of colloid–polymer systems and hard sphere systems in the dilute limit, but fails in giving correct three-body depletion interactions for hard sphere systems at larger volume fractions.

Acknowledgments

We thank the referee for bringing our attention to [13, 22]. This work is supported by the National Nature Science Foundation of China under grand Nos 19825113, 90103035 and 10174041 and Shanghai Science and Technology Committee.

Appendix. Derivation of formula (5)

Under the AO approximation, the formula (5) can be derived in the following way. Consider the configuration show in figure 1: the centre of the big spheres 1, 2 and 3 are $(0, 0, 0)$, $(-h, R, 0)$ and $(-h, -R, 0)$ respectively. Here $h = D + L$ and $L = \sqrt{3}R$ is the smallest value of h when the three spheres are touching. According to formula (4), when the distance between sphere 1 and spheres 2 and 3 is larger then $2a$, the force on sphere 1 is zero; this means that there is a maximum of h beyond which the interaction between sphere 1 and spheres 2 and 3 is absent. The value is

$$L_2 = \sqrt{(R + 2a)(3R + 2a)}.$$

When h is decreased from L_2, the force is no longer zero. The many-body effects are still absent because sphere 2 and sphere 3 exclude a portion of the surface of sphere 1 from reaching the small spheres independently. When h is further decreased to the value $L_1 = R+a+\sqrt{(2R + a)a}$, the exclusion effects from spheres 2 and 3 are correlated so that the many-body effect shows up.

When $L_1 < h \leqslant L_2$, the force is simply the sum of the x-component of the two-body force between sphere 1 and spheres 2 and 3; we only need to derive the force in the case of $L < h \leqslant L_1$. The only nonzero component of the force on sphere 1 is the x-component,

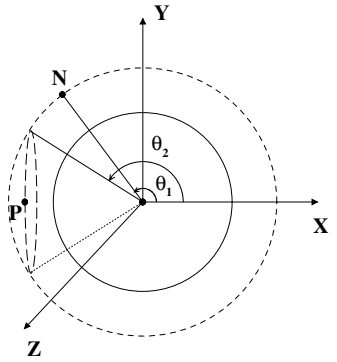

Figure A.1. A portion of figure 1, giving the integration domain of (A.1).

which is

$$F_1 = F_{1x} = -\rho k_B T (R+a)^2 \int \sin\theta \cos\theta \, d\theta \, d\varphi. \tag{A.1}$$

The integration domain of (A.1) includes two parts, S_1 and S_2, shown in figure A.1. The angles θ_1 and θ_2 can easily be determined from geometrical constraints of the AO approximation:

$$\theta_2 = \pi - \arccos \frac{R^2 + h^2}{2h(R+a)},$$

$$\cos\theta_1 = \frac{-h(R^2+h^2)^2 + \sqrt{4(R+a)^2R^2 - (R^2+h^2)R^2}}{2(R+a)(R^2+h^2)^2}.$$

In the domain S_1, the integration interval of ϕ is a function of θ, given by

$$\varphi = \frac{\pi}{2} - \arcsin \frac{h^2 + R^2 + 2(R+a)h\cos\theta}{2(R+a)R\sin\theta}. \tag{A.2}$$

Finally, the integration can be calculated to get

$$F_{S2} = -\frac{3k_BT}{4a^3}\eta \frac{4(R+a)^2h^2 - (R^2+h^2)^2}{4h^2}, \tag{A.3}$$

$$\begin{aligned} F_{S1} &= -4k_BT(R+a)^2\rho \int_{\theta_2}^{\theta_1} \sin\theta\cos\theta \, d\theta \int_0^{\varphi'} d\varphi \\ &= -4k_BT(R+a)^2\rho \int_{\theta_2}^{\theta_1} \sin\theta\cos\theta \left[\frac{\pi}{2} - \arcsin\frac{h^2+R^2+2(R+a)h\cos\theta}{2(R+a)R\sin\theta}\right] d\theta \\ &= \frac{3k_BT}{a^3}\eta(R+a)^2 \int_{\theta_1}^{\theta_2} \sin\theta\cos\theta \left[\frac{\pi}{2} - \arcsin\frac{h^2+R^2+2(R+a)h\cos\theta}{2(R+a)R\sin\theta}\right] d\theta. \end{aligned} \tag{A.4}$$

References

[1] Asakura S and Oosawa F 1954 *J. Chem. Phys.* **22** 1255
[2] Ye X, Narayanan T, Tong P, Huang J S, Lin M Y, Carvalho B L and Fetters L J 1996 *Phys. Rev.* E **54** 6500
[3] Ohshima Y N, Sakagami H, Okumoto K, Tokoyoda A, Igarashi T, Shintaku K B, Toride S, Sekino H, Kabuto K and Nishio I 1997 *Phys. Rev. Lett.* **78** 3963

[4] Kaplan P D, Faucheux L P and Libchaber A J 1994 *Phys. Rev. Lett.* **73** 2793
[5] Dinsmore A D, Yodh A G and Pine D J 1996 *Nature* **383** 259
[6] Dinsmore A D, Wong D T, Nelson P and Yodh A G 1998 *Phys. Rev. Lett.* **80** 409
[7] Crocker J C, Matteo J A, Dinsmore A D and Yodh A G 1999 *Phys. Rev. Lett.* **82** 4352
[8] Biben T, Bladon P and Frenkel D 1996 *J. Phys.: Condens. Matter* **8** 10799–821
[9] Dickman R, Attard P and Simonnian V 1997 *J. Chem. Phys.* **107** 205
[10] Gast A P, Hall C K and Russel W B 1986 *J. Colloid Interface Sci.* **109** 161
[11] Dijkstra M and Frenkel D 1994 *Phys. Rev. Lett.* **72** 298
[12] Dijkstra M, van Roij R and Evans R 1999 *Phys. Rev.* E **59** 5744
[13] Brader J M, Dijkstra M and Evans R 2001 *Phys. Rev.* E **63** 041405
[14] Goulding D and Melchionna S 2001 *Phys. Rev.* E **64** 011403
[15] Rosenfeld Y 1993 *J. Chem. Phys.* **98** 8126
[16] Götzelmann B, Evans R and Dietrich S 1998 *Phys. Rev.* E **57** 6785
[17] Attard P 1989 *J. Chem. Phys.* **91** 3083
[18] Bennett C H 1976 *J. Comput. Phys.* **22** 245
see also Allen M P and Tildesley D J 1994 *Computer Simulation of Liquids* (Oxford: Clarendon) chapter 7
[19] Li W, Xue S and Ma H R 2001 *J. Shanghai Jiaotong University* E **6** 126
[20] Li W and Ma H 2002 *Phys. Rev.* E **66** 61407
[21] Li W and Ma H 2003 *J. Chem. Phys.* **119** 585
[22] Dijkstra M and van Roij R 2002 *Phys. Rev. Lett.* **89** 208303